

Efficient removal of pharmaceutical contaminants using laccase immobilized on activated coal derived desde cashew nut shells: Thermodynamic, Kinetic and Calorimetry study

CA Guerrero-Fajardo¹, L. Giraldo², JC Moreno-Pirajan³

¹ Facultad de Ciencias, Departamento de Química, Aprena Research Group, Carrera 30 No. 45-03, Edificio Uriel Gutiérrez, Ciudad Universitaria, Universidad Nacional de Colombia, Bogotá Sede, Bogotá, 111321, Colombia, Sur América.

² Facultad de Ciencias, Departamento de Química, Grupo de Calorimetría, Carrera 30 No. 45-03, Edificio Uriel Gutiérrez, Ciudad Universitaria, Universidad Nacional de Colombia, Bogotá Sede, Bogotá, 111321, Colombia, Sur América.

³ Facultad de Ciencias, Departamento de Química, Grupo de Investigación en Sólidos Porosos y Calorimetría Aplicada, Carrera 1 No 18 A 12, Universidad de los Andes, Bogotá, 111711, Colombia, Sur América.

Corresponding author: jumoreno@uniandes.edu.co

Abstract

This study details the removal of diclofenac, amoxicillin, and carbamazepine using granular activated carbons (ACs) derived from cashew nut shells. Laccase enzyme impregnation was achieved using three activating agents (KOH, NaOH, ZnCl₂), resulting in bioadsorbents labeled as LAC-x. Fourier transform infrared spectroscopy (FTIR) confirmed enzyme immobilization. Optimal conditions were pH 5, 30°C, and a laccase content of 2.5 mg mL⁻¹. Laccase immobilization increased from 10°C to 30°C, with values of 63.3 to 53.4 U g⁻¹, respectively. Decreased immobilization at 40-50°C was observed due to restricted enzyme access in porous structures. Immersion interactions exhibited spontaneous exothermic behavior following Langmuir isotherms and pseudo-first-order kinetics. This enzymatic removal system offers scalable potential, representing a significant advancement in pharmaceutical disposal research.

Keywords: Pharmaceutical contaminants, Thermodynamics, Adsorption, Immersion Calorimetry, Enzyme Laccase.

1. Introduction

The presence of emerging compounds poses a significant threat to global environmental and human health equilibrium. These compounds, spanning pharmaceuticals, personal care products, pesticides, and industrial byproducts, infiltrate ecosystems via various pathways including wastewater discharge, agricultural practices, and improper disposal [1–13]. Their impact on aquatic organisms, ecosystems, and human health is well-documented, ranging from disruptions in biological processes to hormonal disorders [14–21].

Numerous removal methods, encompassing physical, chemical, and biological approaches, have been developed to mitigate this issue, with biological methods like biodegradation and bioadsorption gaining traction due to their efficacy and eco-friendliness [22–28]. Among bioadsorbents, activated carbon derived from cashew nut shells shows promise, leveraging the fruit's abundant waste to produce a material with high surface area and porosity, ideal for adsorbing organic pollutants [29–45].

Immobilizing laccase on activated carbon further enhances contaminant degradation, but thorough kinetic, thermodynamic, and calorimetric studies are needed to understand this interaction fully and optimize removal processes. Therefore, this research aims to address emerging compound contamination by employing bioadsorbents based on laccase-immobilized activated carbon, focusing on amoxicillin, diclofenac, and carbamazepine as probe molecules (AMO, DFC, CBZ). The study also intends to explore the broader applications and benefits of this approach while emphasizing the necessity for future research to develop sustainable solutions for emerging contaminant removal.

2. Methodology and materials

The chemical activation method was used with three different activating agents to explore the capacity to retain the laccase enzyme and its subsequent effectiveness in the adsorption-degradation of the emerging compounds used in this research: KOH, NaOH and ZnCl₂.

2.1 Activation methods [46-59]

The activated carbons from cashew nut shells were prepared by chemical activation using KOH (ACK), NaOH (ACN), and ZnCl₂ (ACZ) under the conditions suggested in the literature and by our laboratory experience.

2.1.2 Textural characterization of activated carbons

The characterization of the specific surface area and pore texture of the synthesized activated carbons was carried out by nitrogen adsorption-desorption analysis at -196 °C, using the AutosorbiQ St equipment (Anton Paar, Boynton Beach, FL, US). The specific surface area related to micropores, S_{BET} (m²g⁻¹), was determined using the BET (Brunauer-Emmett-Teller) method for calculation [60]. The mesoporous pore size distribution, PSD, was estimated using the Barret-Joyner-Halenda (BJH) calculation method [60,61]. To estimate the PSD of the micropores, the nonlocal density functional theory (NLDFT) calculation method was employed using the SAIEUS® software [62]. In addition, the surface area, S_{NLDFT} (m²g⁻¹), the total pore volume, V_{tot} (m³g⁻¹), and the micropore volume, V_{mic} (m³g⁻¹), were also determined using the NLDFT method integrating the PSD over the entire range of pore sizes. Finally, the mesopore volume, V_{mesopore} (m³g⁻¹), was calculated as the difference between V_{tot} and V_{mic}.

2.2 Fixation of laccase on activated carbon

The experimental procedure followed established methodologies with slight modifications based on prior research and laboratory experience. In summary, activated carbon (AC) was mixed with a laccase enzyme solution and incubated at 30°C and 250 rpm for six hours. After centrifugation and rinsing steps to remove unbound enzyme, immobilized laccase activity was determined by subtracting initial activity. Further analyses, including pH, temperature, stability, enzyme concentrations, and optimal parameters for contaminant removal, were conducted on resulting samples [63-65].

2.2.1 Enzymatic Assay

Enzymatic activity was assessed by monitoring the oxidation of ABTS, a substrate for laccase, for both free and immobilized enzyme forms. Absorbance increase at 425 nm, using an extinction coefficient of ε = 36,000 M⁻¹cm⁻¹, was recorded at room temperature with a double-beam Aligent Cary 3500 Compact UV-Vis spectrophotometer. One laccase activity unit was defined as the enzyme amount oxidizing one micromole of ABTS per minute under standard assay conditions: pH = 5 buffer, 0.5 mM ABTS, and 2 mg mL⁻¹ enzyme concentration. The color change to blue during the process indicated successful ABTS oxidation [63-65].

$$\text{Free laccase activity (U.mL}^{-1}\text{)} = \frac{\Delta\text{abs} \times D_f \times R_v}{\epsilon \times t \times E_v} \quad (1)$$

$$\text{Immobilized laccase activity (Ug}^{-1}\text{)} = \frac{\Delta\text{abs} \times D_f \times R_v}{\epsilon \times t \times M_{\text{carrier}}} \quad (2)$$

The variables in the above equations are defined as follows: Δabs represents the absorbance of ABTS⁺, D_f is the dilution factor, R_v represents the reaction volume in milliliters, ε denotes the extinction coefficient of ABTS⁺, t represents the duration of the reaction in minutes, M_{carrier} indicates the mass of the carrier used for laccase immobilization in grams and E_v represents the volume of the enzyme in milliliters.

2.3 FTIR, Boehm titrations

The chemical structure of the prepared solids was determined using FTIR, specifically a Nicolet™ iSTM 5 FTIR instrument coupled to iD7 ATR. IR spectra were obtained with a resolution of 2 cm⁻¹ (400 to 4000 cm⁻¹). To assess laccase enzyme fixation effectiveness, Boehm titrations were performed to quantify surface functional groups, including phenolic (–OH), carboxylic (–COOH), and carbonyl (C=O) groups typical of activated carbons. Basic

and acidic sites were evaluated using NaHCO_3 , Na_2CO_3 , and NaOH solutions (0.05 M), mixed with activated carbon and stirred for 72 hours. Subsequently, excess solution was quantified by back-titration using NaOH (0.025 M) for basic sites and HCl (0.025 M) for acidic sites [66-67].

2.4 Determination of the point of zero charge (pH_{PZC}).

Activated carbon surfaces exhibit varying acidity levels based on precursor origin and activation method. The point of zero charge (pH_{PZC}) was determined to assess this property, as shown in Fig 1. Results indicate acidic pH_{PZC} values of 5.0, 4.5, and 6.0 for KOH , NaOH , and ZnC_{12} activated carbons, respectively. Chemical activation produces acidic oxygenated surface groups.

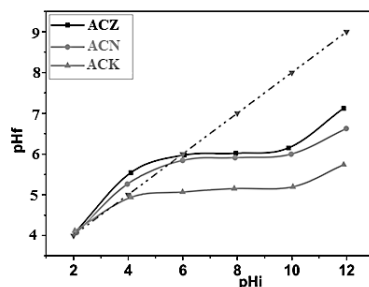


Fig 1. Results obtained in the determination of pH_{PZC} for ACK, ACN and ACZ

2.5 HPLC measurements

In this study, diclofenac (DCF), carbamazepine (CBZ), and amoxicillin (AMO) were used as probe molecules to investigate adsorption-degradation. High-performance liquid chromatography (HPLC) using a Merck-Hitachi D-7000 instrument determined pharmaceutical degradation. Zorbax SB-Aq column (150 mm \times 4.6 mm, 5 μm) with gradient elution was employed. Sample volume injected was 10 μL . Mobile phase consisted of 0.1% trifluoroacetic acid in MQ water (eluent A) and methanol (eluent B), with a gradient program from 40% to 100% B over 1 to 5 minutes. Flow rate was 1 mL min^{-1} . Calibration showed linearity between 5 and 100 $\mu\text{g mL}^{-1}$ for DCF, AMO, and CBZ. Degradation of these compounds involved adding 250 mg of LAC-x to 0.075 L matrix containing 100 mg L^{-1} of pharmaceutical molecules, stirring continuously at 150 rpm. Supernatant samples were collected every 30 minutes for analysis by HPLC. Additionally, adsorption experiments without immobilization were conducted under similar conditions [66-70]

2.6 Adsorption, kinetics and thermodynamics studies.

Several models have been employed to describe adsorption processes, using variables like q_e (amount adsorbed per gram of adsorbent at equilibrium, mg g^{-1}) and C_e (solute concentration in solution at equilibrium, mg L^{-1}) to determine adsorption characteristics. Langmuir and Freundlich models were utilized, each with its non-linear and linear equations. These models were applied to interpret the adsorption of pharmaceutical molecules from aqueous solution on bioadsorbents, with fitting parameters determined from original adsorption data. Subsequently, adsorption kinetics of DCF, AMO, and CBZ were analyzed using pseudo-first order (PFO), pseudo-second order (PSO), and intraparticle diffusion (IPD) models. The suitability of each model was assessed using the coefficient of determination (R^2). In kinetic experiments, 200 mg of each adsorbent was added to 50 mL of solution containing the molecules, stirred at 250 rpm. Concentrations were measured at specific intervals, and the amount adsorbed at equilibrium (q_e) was calculated. Additionally, the Elovich model was applied. Thermodynamic parameters including Gibbs free energy change (ΔG°), enthalpy change (ΔH°), and entropy change (ΔS°) were calculated to understand the adsorbate-adsorbent interaction. These parameters were determined using the classical equations of thermodynamics, with ΔG° related to the thermodynamic adsorption equilibrium constant (K_c°), universal gas constant (R), and temperature (T). The relationship between ΔH° , ΔS° , and K_c° was established using the linearized van't Hoff equation [71-75].

2.7 The immersion enthalpy of the bioadsorbents synthesized in this research.

DFC, CBZ, and AMO were analyzed for their relationship with bioadsorbents using a locally constructed microcalorimeter equipped with thermopiles, recording thermal changes during interaction with solvents. Electrical calibration was performed [76-82].

3. Results

FTIR results for activated carbons without laccase showed different molecular vibrations. It was established that impregnation with the laccase enzyme caused subtle changes in some of the FTIR bands. Electrostatic and hydrophobic interactions facilitate the adsorption of enzymes on activated carbon under certain conditions. Generally, the laccase enzyme tends to have a basic character, which complemented the acidic nature of the prepared carbons, favoring the fixation of enzymes [65, 83].

Textural characterization

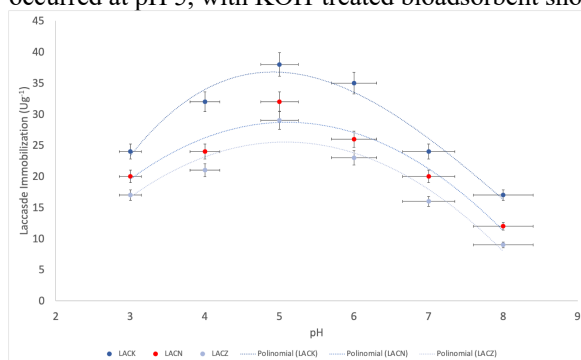
Textural parameters in Table 1 demonstrate KOH activation yields highest surface area and pore volume compared to NaOH and ZnCl₂. KOH-treated carbons display well-developed specific surface and micropores, evident from micropore volume exceeding total volume and S_{NLDFT} exceeding S_{BET}. ZnCl₂ activation produces a deeper microporous structure with lower pore volume and surface area. The average pore diameter of KOH-treated carbon is smaller, confirming mainly microporous nature. PSD analysis reveals varied pore sizes, with KOH and NaOH showing concentrated micropores. These findings validate activation efficiency and the impact of activating agents. Notably, ZnCl₂ maintains good N₂ adsorption capacity while preserving microporosity, crucial for practical applications.

Table 1. Textural characterization by N₂ adsorption isotherms at -196 °C

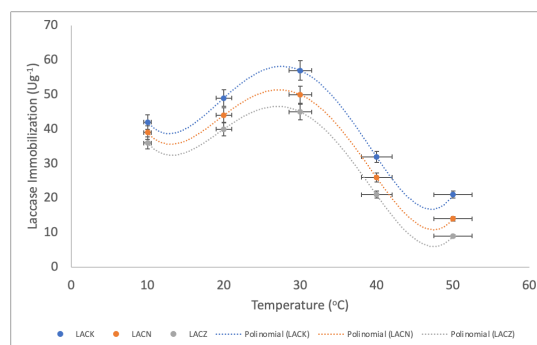
Sample	S _{BET} m ² g ⁻¹	S _{NLDFT} m ² g ⁻¹	Average Particle Size nm	Total Pore Volume cm ³ g ⁻¹	Mesopore Volume cm ³ g ⁻¹	Micropore Volume cm ³ g ⁻¹	Microporosity (%)
ACK	1300.	1343	1.9	1.46	0.42	0.99	70.2
ACN	1100	1054	2.2	1.09	0.31	0.88	74.0
ACZ	800	775	2.5	0.45	0.06	0.31	83.8

Enzymatic immobilization

The adsorption method immobilized laccase enzyme on activated carbons (AC's) prepared in this study. To optimize immobilization, pH and temperature effects were studied. Figs 2a-d illustrate pH, temperature, enzyme concentration, and immobilization performance. Laccase immobilization increased progressively from pH 3 to 5, reaching maxima at pH 5. Temperature between 10°C to 30°C favored immobilization, with a decline at higher temperatures [63-65]. Enzyme concentration between 1.0 to 2.0 mg mL⁻¹ showed increased immobilization, but higher concentrations had no effect due to limited surface sites. Optimal immobilization occurred at pH 5, with KOH-treated bioadsorbent showing the highest yield at 77.5%.



(a)



(b)

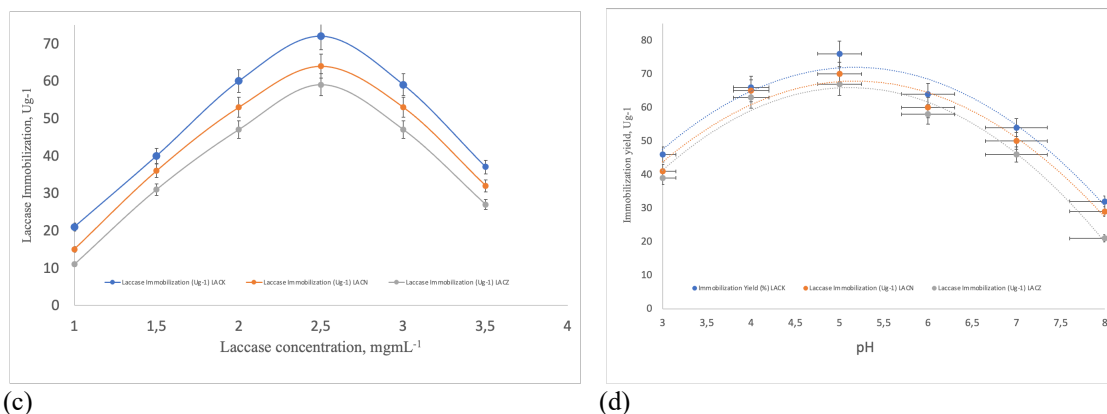


Fig 2. Effect of varying the pH level (a), temperatures (b) and concentrations of the laccase enzyme (c) on the immobilization and efficiency of the process (d).

Adsorption studies: isotherms, kinetics and thermodynamics.

The experimental data of fitting probe molecules (amoxicillin, diclofenac and carbamazepine – AMO, DCF, CBZ) in bioadsorbents (carbons activated with laccase enzyme – LAC-x) used Langmuir and Freundlich isotherms, as shown in the results reported. in Table 2a, 2b and 2c. The Langmuir model showed superior fit with high correlation coefficients (around 0.99) for all bioadsorbents. The Freundlich models had R^2 values further from unity, indicating monolayer formation. LACK showed the highest sorption capacity, with DCF being the most adsorbed (387.7 mg g^{-1}), followed by CBZ (344.3 mg g^{-1}) and AMO (324.6 mg g^{-1}). R_L values ($0 < R_L < 1$) indicate favorable adsorption, while high K_L values suggest a strong affinity between pharmaceutical molecules and bioadsorbents. Finally, it is worth highlighting that the data obtained here are in total agreement taking into account the chemical characteristics of the bioadsorbents and the corresponding chemical characteristics of the emerging compound.

Table 2a Fitting experimental data to amoxicillin (AMO) adsorption models

Samples	Langmuir				Freundlich		
	R_L	q_{max}	$K_L(\text{Lmg}^{-1})$	R^2	$K_F (\text{mg} \cdot \text{g}^{-1} \cdot \text{L}^{-1})$	nF	R^2
LACK	0.794	324.6	0.7564	0.999	312.2	10.432	0.968
LACN	0.753	309.3	0.6845	0.993	287.4	8.432	0.953
LACZ	0.654	267.1	0.5313	0.996	212.8	7.982	0.934

Table 2b. Fitting experimental data to diclofenac (DCF) adsorption models

Samples	Langmuir				Freundlich		
	R_L	q_{max}	$K_L(\text{Lmg}^{-1})$	R^2	$K_F (\text{mg} \cdot \text{g}^{-1} \cdot \text{L}^{-1})$	nF	R^2
LACK	0.898	387.7	0.9657	0.991	312.2	16.546	0.929
LACN	0.876	342.3	0.8721	0.992	287.4	13.432	0.976
LACZ	0.865	301.4	0.6542	0.997	212.8	11.954	0.959

Table 2c. Fitting experimental data to carbamazepine (CBZ) adsorption models

Samples	Langmuir				Freundlich		
	R_L	q_{max}	$K_L(\text{Lmg}^{-1})$	R^2	$K_F (\text{mg} \cdot \text{g}^{-1} \cdot \text{L}^{-1})$	nF	R^2
LACK	0.843	344.3	0.8725	0.998	312.2	12.983	0.978
LACN	0.804	321.7	0.7821	0.996	287.4	10.231	0.967
LACZ	0.786	287.3	0.5987	0.992	212.8	9.432	0.945

Another hand, Pseudo-first-order (PFO) and pseudo-second-order (PSO) kinetics were utilized to explore adsorption mechanisms and intermolecular forces, including covalent and ion exchange. PFO describes

reversible physical adsorption, while PSO involves chemical bonds. Intraparticle diffusion (IPD) model elucidates rate-limiting steps. Figs 3 depicts fits to PFO, PSO, IPD, and Elovich models for tested pharmaceutical compounds. Results align with PFO kinetics, indicating physisorption limits adsorption. Three linear segments observed in IPD modeling suggest multi-stage adsorption, involving external diffusion, lower diffusion into porous structure, and subsequent saturation of reactive sites. Overall, adsorption of pharmaceuticals on bioadsorbents involves physisorption and chemisorption mechanisms, with IPD revealing three sequential steps: film diffusion, gradual adsorption, and equilibrium [70-81].

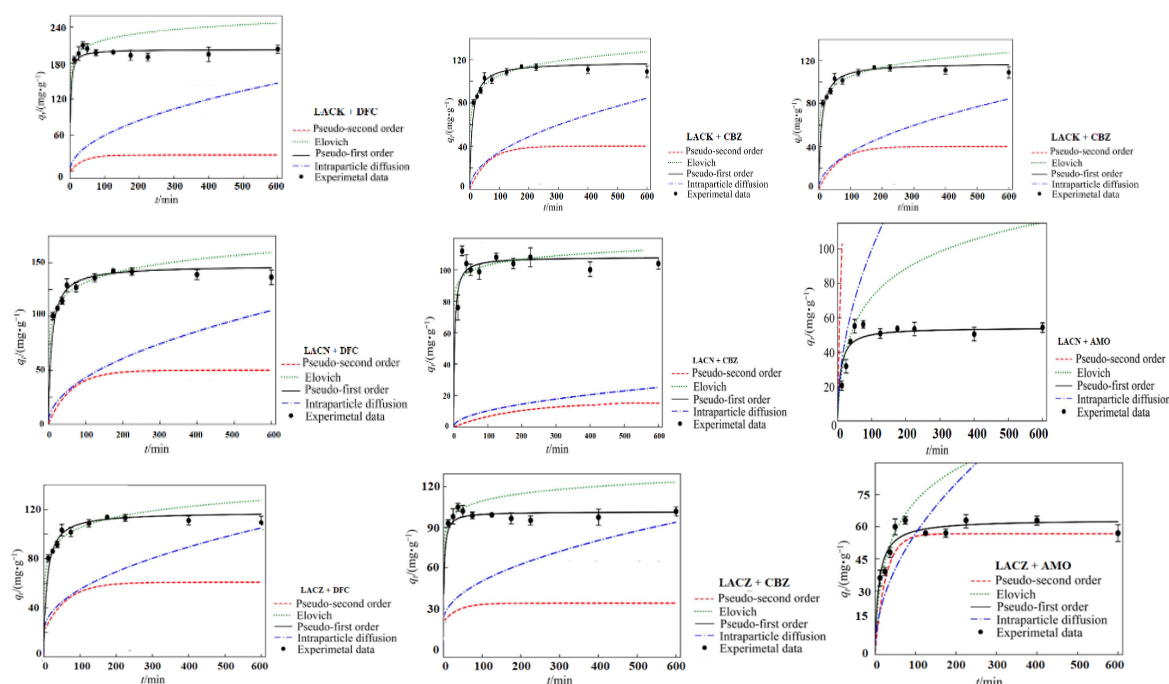


Fig 3. Kinetic models applied to the adsorption isotherms of PFO, PSO, IDF and Elovich: comparative analysis and adjustment.

The evaluation of the thermodynamic parameters of the pharmaceutical compounds in the bioadsorbents were evaluated. The results showed that the ΔG° values decrease with increasing temperature, indicating a beneficial influence of temperature on the adsorption efficiency. Negative ΔG° values measured at four different temperatures indicate spontaneous adsorption of pharmaceutical compounds and all biosorbents. Positive values of ΔH° suggest an endothermic adsorption process. Positive values of ΔS° indicate a stable and random adsorption process [75, 82].

Calorimetric results analysis

Calorimetric studies were performed to explore the interactions between the bioadsorbents and the pharmaceutical molecules used in the study. The immersion enthalpy, a thermodynamic parameter correlated with pore structure and surface chemistry, was analyzed. The enthalpies of immersion in water and various solutions. These values varied depending on the type of interaction established between the bioadsorbent and the pharmaceutical molecules. In particular, the LACK biosorbent system exhibited the highest values for the thermodynamic variables, indicating greater compatibility with the tested pharmaceutical molecules [82-84]. The immersion calorimetric curves of LACK, LACN and LACZ in DFC, CBZ, AMO, benzene and water at 100 ppm (potential vs. time) were determined. The area under the curve represents the amount of heat produced by the solid-liquid contact. The thermograms facilitated the evaluation of immersion enthalpies for DFC, CBZ, AMO, benzene, and water in the synthesized bioadsorbents. Immersion enthalpies were predominantly

negative, indicating an exothermic process. LACN showed a hydrophilic nature, evidenced by the Hf factor exceeding unity and high enthalpies of immersion in water. This behavior was attributed to the -OH groups introduced during the chemical activation process and reinforced by the fixation of enzymes on the surface of the bioadsorbent.

The enzyme laccase, with various functional groups including -NH₂, -COOH, and -OH, could influence the surface of activated carbon when attached to carbon treated with KOH or NaOH. This could introduce a localized polarity, reinforcing the hydrophilic behavior. The hydrophilic factor was correlated with the structure and characteristics of the molecules. Diclofenac sodium, carbamazepine, and amoxicillin interacted primarily through ion-dipole interactions, hydrogen bonding, and dissolution in aqueous solutions.

The interaction between LACK and DFC exhibited the highest immersion enthalpies, followed by the LACK-CBZ and LACK-AMO interactions. This trend aligned with findings from previous research. LACK acid-type activated carbon showed stronger interactions with pharmaceutical molecules compared to other bioadsorbents.

4. Conclusions

In this study, activated carbon was derived from cashew nut shells using KOH, NaOH, and ZnCl₂ as activating agents, with laccase enzyme immobilization to create bioadsorbents. These were tested for adsorption capacity of diclofenac sodium, carbamazepine, and amoxicillin, alongside kinetics, thermodynamics, and calorimetric analysis. Results indicate all bioadsorbents conform well to the Langmuir model, with LACK exhibiting the highest adsorption capacity: 387.7 mgg⁻¹ for DFC, 344.3 mgg⁻¹ for CBZ, and 3245.6 mgg⁻¹ for AMO, surpassing values reported in literature. Adsorption followed the PFO model, with IPD analysis revealing a three-step process, likely involving some chemical interaction. Thermodynamic evaluation, particularly Gibbs free energy, affirmed spontaneity. Calorimetric data confirmed exothermic enthalpy, with LACK-DFC exhibiting the highest value at 158.7 kJmol⁻¹, followed by LACK-CBZ at 137.4 kJmol⁻¹, and LACK-AMO at 125.8 kJmol⁻¹. Overall, the research highlights the potential of agricultural waste-derived bioadsorbents in efficiently removing emerging compounds, with spontaneous adsorption demonstrated via calorimetric analysis, supporting scalability.

Acknowledgments

The authors thank you MinCiencias by economic funds approved by the projects titled "Biocatalysts supported on porous and graphenic materials for the degradation of contaminants emerging from the manufacture of plastics and the use of agrochemicals", Contract No. CT ICETEX 2023- 0814 CD 1101- 890-82458. The authors thank the Framework Agreement between Universidad de Los Andes and Universidad Nacional de Colombia—Bogotá and the act of agreement established between the Departments of Chemistry of both institutions. The Prof. Dr. Juan Carlos Moreno- Piraján also thank the grant project No. INV-2023-162- 2735 by the Faculty of Sciences (Universidad de los Andes, Bogotá, Colombia).

References

1. Benotti, M.J., Brownawell, B.J.: Microbial degradation of pharmaceuticals in estuarine and coastal seawater. *Environmental Pollution*. 157, 994–1002 (2009). <https://doi.org/10.1016/j.envpol.2008.10.009>
2. Berkner, S., Thierbach, C.: Biodegradability and transformation of human pharmaceutical active ingredients in environmentally relevant test systems. *Environmental Science and Pollution Research*. 21, 9461–9467 (2014). <https://doi.org/10.1007/s11356-013-1868-6>
3. Bijekar, S., Padariya, H.D., Yadav, V.K., Gacem, A., Hasan, M.A., Awwad, N.S., Yadav, K.K., Islam, S., Park, S., Jeon, B.-H.: The State of the Art and Emerging Trends in the Wastewater Treatment in Developing Nations. *Water (Basel)*. 14, 2537 (2022). <https://doi.org/10.3390/w14162537>
4. Del Rosario, K.L., Mitra, S., Humphrey, C.P., O'Driscoll, M.A.: Detection of pharmaceuticals and other personal care products in groundwater beneath and adjacent to onsite wastewater treatment systems in a coastal plain shallow aquifer. *Science of The Total Environment*. 487, 216–223 (2014). <https://doi.org/10.1016/j.scitotenv.2014.03.135>

5. Do, Q.T.T., Otaki, M., Otaki, Y., Tushara, C., Sanjeeva, I.W.: Pharmaceutical Contaminants in Shallow Groundwater and Their Implication for Poor Sanitation Facilities in Low-Income Countries. *Environ Toxicol Chem.* 41, 266–274 (2022). <https://doi.org/10.1002/etc.5110>
6. Mastrocicco, M., Colombani, N.: The Issue of Groundwater Salinization in Coastal Areas of the Mediterranean Region: A Review. *Water (Basel)*. 13, 90 (2021). <https://doi.org/10.3390/w13010090>
7. Sacher, F., Lange, F.T., Brauch, H.-J., Blankenhorn, I.: Pharmaceuticals in groundwaters. *J Chromatogr A*. 938, 199–210 (2001). [https://doi.org/10.1016/S0021-9673\(01\)01266-3](https://doi.org/10.1016/S0021-9673(01)01266-3)
8. Vystavna, Y., Le Coustumer, P., Huneau, F.: Monitoring of trace metals and pharmaceuticals as anthropogenic and socio-economic indicators of urban and industrial impact on surface waters. *Environ Monit Assess.* 185, 3581–3601 (2013). <https://doi.org/10.1007/s10661-012-2811-x>
9. Ahmed, M.J., Hameed, B.H.: Removal of emerging pharmaceutical contaminants by adsorption in a fixed-bed column: A review. *Ecotoxicol Environ Saf.* 149, 257–266 (2018). <https://doi.org/10.1016/j.ecoenv.2017.12.012>
10. Diniz, V., Gasparini Fernandes Cunha, D., Rath, S.: Adsorption of recalcitrant contaminants of emerging concern onto activated carbon: A laboratory and pilot-scale study. *J Environ Manage.* 325, 116489 (2023). <https://doi.org/10.1016/j.jenvman.2022.116489>
11. Diniz, V., Rath, G., Rath, S., Araújo, L.S., Cunha, D.G.F.: Competitive kinetics of adsorption onto activated carbon for emerging contaminants with contrasting physicochemical properties. *Environmental Science and Pollution Research.* 29, 42185–42200 (2022). <https://doi.org/10.1007/s11356-021-16043-2>
12. Genç, N., Durna, E., Erkişi, E.: Optimization of the adsorption of diclofenac by activated carbon and the acidic regeneration of spent activated carbon. *Water Science and Technology.* 83, 396–408 (2021). <https://doi.org/10.2166/wst.2020.577>
13. Ouyang, J., Zhou, L., Liu, Z., Heng, J.Y.Y., Chen, W.: Biomass-derived activated carbons for the removal of pharmaceutical micropollutants from wastewater: A review. *Sep Purif Technol.* 253, 117536 (2020). <https://doi.org/10.1016/j.seppur.2020.117536>
14. Ahn, Y.-T., Cho, D.-W., Kabra, A.N., Ji, M.-K., Yoon, Y., Choi, J., Choi, I.-H., Kang, J.-W., Kim, J.R., Jeon, B.-H.: Removal of Iopromide and Its Intermediates from Ozone-Treated Water Using Granular Activated Carbon. *Water Air Soil Pollut.* 226, 346 (2015). <https://doi.org/10.1007/s11270-015-2594-0>
15. Anumol, T., Sgroi, M., Park, M., Roccaro, P., Snyder, S.A.: Predicting trace organic compound breakthrough in granular activated carbon using fluorescence and UV absorbance as surrogates. *Water Res.* 76, 76–87 (2015). <https://doi.org/10.1016/j.watres.2015.02.019>
16. Borrull, J., Colom, A., Fabregas, J., Borrull, F., Pocurull, E.: Presence, behaviour and removal of selected organic micropollutants through drinking water treatment. *Chemosphere.* 276, 130023 (2021). <https://doi.org/10.1016/j.chemosphere.2021.130023>
17. Bourgin, M., Beck, B., Boehler, M., Borowska, E., Fleiner, J., Salhi, E., Teichler, R., von Gunten, U., Siegrist, H., McArdell, C.S.: Evaluation of a full-scale wastewater treatment plant upgraded with ozonation and biological post-treatments: Abatement of micropollutants, formation of transformation products and oxidation by-products. *Water Res.* 129, 486–498 (2018). <https://doi.org/10.1016/j.watres.2017.10.036>
18. Calisto, V., Ferreira, C.I.A., Oliveira, J.A.B.P., Otero, M., Esteves, V.I.: Adsorptive removal of pharmaceuticals from water by commercial and waste-based carbons. *J Environ Manage.* 152, 83–90 (2015). <https://doi.org/10.1016/j.jenvman.2015.01.019>
19. Campinas, M., Silva, C., Viegas, R.M.C., Coelho, R., Lucas, H., Rosa, M.J.: To what extent may pharmaceuticals and pesticides be removed by PAC conventional addition to low-turbidity surface waters and what are the potential bottlenecks? *Journal of Water Process Engineering.* 40, 101833 (2021). <https://doi.org/10.1016/j.jwpe.2020.101833>
20. Cantoni, B., Turolla, A., Wellmitz, J., Ruhl, A.S., Antonelli, M.: Perfluoroalkyl substances (PFAS) adsorption in drinking water by granular activated carbon: Influence of activated carbon and PFAS characteristics. *Science of The Total Environment.* 795, 148821 (2021). <https://doi.org/10.1016/j.scitotenv.2021.148821>
21. de Ridder, D.J., Verliefde, A.R.D., Heijman, S.G.J., Verberk, J.Q.J.C., Rietveld, L.C., van der Aa, L.T.J., Amy, G.L., van Dijk, J.C.: Influence of natural organic matter on equilibrium adsorption of neutral and charged pharmaceuticals onto activated carbon. *Water Science and Technology.* 63, 416–423 (2011). <https://doi.org/10.2166/wst.2011.237>
22. Deniere, E., Chys, M., Audenaert, W., Nopens, I., Van Langenhove, H., Van Hulle, S., Demeestere, K.: Status and needs for online control of tertiary ozone-based water treatment: use of surrogate correlation

- models for removal of trace organic contaminants. *Rev Environ Sci Biotechnol.* (2021). <https://doi.org/10.1007/s11157-021-09574-0>
23. Egea-Corbacho, A., Gutiérrez Ruiz, S., Quiroga Alonso, J.M.: Removal of emerging contaminants from wastewater using nanofiltration for its subsequent reuse: Full-scale pilot plant. *J Clean Prod.* 214, 514–523 (2019). <https://doi.org/10.1016/j.jclepro.2018.12.297>
 24. FENT, K., WESTON, A., CAMINADA, D.: Ecotoxicology of human pharmaceuticals. *Aquatic Toxicology.* 76, 122–159 (2006). <https://doi.org/10.1016/j.aquatox.2005.09.009>
 25. Gorito, A.M., Pesqueira, J.F.J.R., Moreira, N.F.F., Ribeiro, A.R., Pereira, M.F.R., Nunes, O.C., Almeida, C.M.R., Silva, A.M.T.: Ozone-based water treatment (O₃, O₃/UV, O₃/H₂O₂) for removal of organic micropollutants, bacteria inactivation and regrowth prevention. *J Environ Chem Eng.* 9, 105315 (2021). <https://doi.org/10.1016/j.jece.2021.105315>
 26. Guillossou, R., Le Roux, J., Brosillon, S., Mailler, R., Vulliet, E., Morlay, C., Nauleau, F., Rocher, V., Gaspéri, J.: Benefits of ozonation before activated carbon adsorption for the removal of organic micropollutants from wastewater effluents. *Chemosphere.* 245, 125530 (2020). <https://doi.org/10.1016/j.chemosphere.2019.125530>
 27. Bernal, V., Giraldo, L., Moreno-Piraján, J.: Physicochemical Properties of Activated Carbon: Their Effect on the Adsorption of Pharmaceutical Compounds and Adsorbate–Adsorbent Interactions. *C (Basel).* 4, 62 (2018). <https://doi.org/10.3390/c4040062>
 28. Dias, J.M., Alvim-Ferraz, M.C.M., Almeida, M.F., Rivera-Utrilla, J., Sánchez-Polo, M.: Waste materials for activated carbon preparation and its use in aqueous-phase treatment: A review. *J Environ Manage.* 85, 833–846 (2007). <https://doi.org/10.1016/j.jenvman.2007.07.031>
 29. García-Mateos, F.J., Ruiz-Rosas, R., Marqués, M.D., Cotoruelo, L.M., Rodríguez-Mirasol, J., Cordero, T.: Removal of paracetamol on biomass-derived activated carbon: Modeling the fixed bed breakthrough curves using batch adsorption experiments. *Chemical Engineering Journal.* 279, 18–30 (2015). <https://doi.org/10.1016/j.cej.2015.04.144>
 30. Gómez-Avilés, A., Sellaoui, L., Badawi, M., Bonilla-Petriciolet, A., Bedia, J., Belver, C.: Simultaneous adsorption of acetaminophen, diclofenac and tetracycline by organo-sepiolite: Experiments and statistical physics modelling. *Chemical Engineering Journal.* 404, 126601 (2021). <https://doi.org/10.1016/j.cej.2020.126601>
 31. Akpotu, S.O., Moodley, B.: Application of as-synthesised MCM-41 and MCM-41 wrapped with reduced graphene oxide/graphene oxide in the remediation of acetaminophen and aspirin from aqueous system. *J Environ Manage.* 209, 205–215 (2018). <https://doi.org/10.1016/j.jenvman.2017.12.037>
 32. George Nche, N.-A., Bopda, A., Raoul, D., Tchuifon, T., Ngakou, C.S., Kuete, I.-H.T., Gabche, A.S.: Removal of Paracetamol from Aqueous Solution by Adsorption onto Activated Carbon Prepared from Rice Husk. Available online www.jocpr.com *Journal of Chemical and Pharmaceutical Research.* 2017, 56–68
 33. Coimbra, R.N., Calisto, V., Ferreira, C.I.A., Esteves, V.I., Otero, M.: Removal of pharmaceuticals from municipal wastewater by adsorption onto pyrolyzed pulp mill sludge. *Arabian Journal of Chemistry.* 12, 3611–3620 (2019). <https://doi.org/10.1016/j.arabjc.2015.12.001>
 34. Abdeljaoued, A., Querejeta, N., Durán, I., Álvarez-Gutiérrez, N., Pevida, C., Chahbani, M.: Preparation and Evaluation of a Coconut Shell-Based Activated Carbon for CO₂/CH₄ Separation. *Energies (Basel).* 11, 1748 (2018). <https://doi.org/10.3390/en11071748>
 35. Abdollahzadeh, H., Fazlzadeh, M., Afshin, S., Arfaenia, H., Feizizadeh, A., Poureshgh, Y., Rashtbari, Y.: Efficiency of activated carbon prepared from scrap tires magnetized by Fe₃O₄ nanoparticles: characterisation and its application for removal of reactive blue19 from aquatic solutions. *Int J Environ Anal Chem.* 102, 1911–1925 (2022). <https://doi.org/10.1080/03067319.2020.1745199>
 36. Ahmad, K.S.: *Arachis hypogaea* derived activated carbon steered remediation of Benzimidazole based fungicide adsorbed soils. *Chemistry and Ecology.* 35, 576–591 (2019). <https://doi.org/10.1080/02757540.2019.1600678>
 37. de Franco, M.A.E., de Carvalho, C.B., Bonetto, M.M., Soares, R. de P., Féris, L.A.: Removal of amoxicillin from water by adsorption onto activated carbon in batch process and fixed bed column: Kinetics, isotherms, experimental design and breakthrough curves modelling. *J Clean Prod.* 161, 947–956 (2017). <https://doi.org/10.1016/j.jclepro.2017.05.197>
 38. Ahmed, M.B., Zhou, J.L., Ngo, H.H., Guo, W., Johir, M.A.H., Sornalingam, K.: Single and competitive sorption properties and mechanism of functionalized biochar for removing sulfonamide antibiotics from water. *Chemical Engineering Journal.* 311, 348–358 (2017). <https://doi.org/10.1016/j.cej.2016.11.106>

39. Amin, R., Khorshidi, A., Shojaei, A.F., Rezaei, S., Faramarzi, M.A.: Immobilization of laccase on modified Fe₃O₄@SiO₂@Kit-6 magnetite nanoparticles for enhanced delignification of olive pomace bio-waste. *Int J Biol Macromol.* 114, 106–113 (2018). <https://doi.org/10.1016/j.ijbiomac.2018.03.086>
40. De La Torre, M., Martín-Sampedro, R., Fillat, U., Eugenio, M.E., Blázquez, A., Hernández, M., Arias, M.E., Ibarra, D.: Comparison of the efficiency of bacterial and fungal laccases in delignification and detoxification of steam-pretreated lignocellulosic biomass for bioethanol production. *J Ind Microbiol Biotechnol.* 44, 1561–1573 (2017). <https://doi.org/10.1007/s10295-017-1977-1>
41. Jeong, D., Choi, K.-Y.: Biodegradation of Tetracycline Antibiotic by Laccase Biocatalyst Immobilized on Chitosan-Tripolyphosphate Beads. *Appl Biochem Microbiol.* 56, 306–312 (2020). <https://doi.org/10.1134/S0003683820030047>
42. Kalyani, D., Dhiman, S.S., Kim, H., Jeya, M., Kim, I.-W., Lee, J.-K.: Characterization of a novel laccase from the isolated *Coltricia perennis* and its application to detoxification of biomass. *Process Biochemistry.* 47, 671–678 (2012). <https://doi.org/10.1016/j.procbio.2012.01.013>
43. Patel, S.K.S., Kalia, V.C., Choi, J.-H., Haw, J.-R., Kim, I.-W., Lee, J.K.: Immobilization of Laccase on SiO₂ Nanocarriers Improves Its Stability and Reusability. *J Microbiol Biotechnol.* 24, 639–647 (2014). <https://doi.org/10.4014/jmb.1401.01025>
44. Rekuć, A., Bryjak, J., Szymańska, K., Jarzębski, A.B.: Laccase immobilization on mesostructured cellular foams affords preparations with ultra high activity. *Process Biochemistry.* 44, 191–198 (2009). <https://doi.org/10.1016/j.procbio.2008.10.007>
45. Alvarado-Ramírez, L., Rostro-Alanis, M., Rodríguez-Rodríguez, J., Castillo-Zacarias, C., Sosa-Hernández, J.E., Barceló, D., Iqbal, H.M.N., Parra-Saldívar, R.: Exploring current tendencies in techniques and materials for immobilization of laccases – A review. *Int J Biol Macromol.* 181, 683–696 (2021). <https://doi.org/10.1016/j.ijbiomac.2021.03.175>
46. Ullah, F., Ji, G., Irfan, M., Gao, Y., Shafiq, F., Sun, Y., Ain, Q.U., Li, A.: Adsorption performance and mechanism of cationic and anionic dyes by KOH activated biochar derived from medical waste pyrolysis. *Environmental Pollution.* 314, 120271 (2022). <https://doi.org/10.1016/j.envpol.2022.120271>
47. Singh, J., Bhunia, H., Basu, S.: Adsorption of CO₂ on KOH activated carbon adsorbents: Effect of different mass ratios. *J Environ Manage.* 250, 109457 (2019). <https://doi.org/10.1016/j.jenvman.2019.109457>
48. Shahkarami, S., Azargohar, R., Dalai, A.K., Soltan, J.: Breakthrough CO₂ adsorption in bio-based activated carbons. *Journal of Environmental Sciences.* 34, 68–76 (2015). <https://doi.org/10.1016/j.jes.2015.03.008>
49. Abdel-Ghani, N.T., El-Chaghaby, G.A., ElGammal, M.H., Rawash, E.-S.A.: Optimizing the preparation conditions of activated carbons from olive cake using KOH activation. *New Carbon Materials.* 31, 492–500 (2016). [https://doi.org/10.1016/S1872-5805\(16\)60027-6](https://doi.org/10.1016/S1872-5805(16)60027-6)
50. Wang, J., Kaskel, S.: KOH activation of carbon-based materials for energy storage. *J Mater Chem.* 22, 23710 (2012). <https://doi.org/10.1039/c2jm34066f>
51. Lozano-Castelló, D., Lillo-Ródenas, M.A., Cazorla-Amorós, D., Linares-Solano, A.: Preparation of activated carbons from Spanish anthracite. *Carbon N Y.* 39, 741–749 (2001). [https://doi.org/10.1016/S0008-6223\(00\)00185-8](https://doi.org/10.1016/S0008-6223(00)00185-8)
52. Lillo-Ródenas, M.A., Lozano-Castelló, D., Cazorla-Amorós, D., Linares-Solano, A.: Preparation of activated carbons from Spanish anthracite. *Carbon N Y.* 39, 751–759 (2001). [https://doi.org/10.1016/S0008-6223\(00\)00186-X](https://doi.org/10.1016/S0008-6223(00)00186-X)
53. Perrin, A., Celzard, A., Albinia, A., Jasienko-Halat, M., Maréché, J.F., Furdin, G.: NaOH activation of anthracites: effect of hydroxide content on pore textures and methane storage ability. *Microporous and Mesoporous Materials.* 81, 31–40 (2005). <https://doi.org/10.1016/j.micromeso.2005.01.015>
54. Somna, K., Jaturapitakkul, C., Kajitvichyanukul, P., Chindapasirt, P.: NaOH-activated ground fly ash geopolymer cured at ambient temperature. *Fuel.* 90, 2118–2124 (2011). <https://doi.org/10.1016/j.fuel.2011.01.018>
55. Zhang, D.-W., Zhao, K.-F., Xie, F., Li, H., Wang, D.: Effect of water-binding ability of amorphous gel on the rheology of geopolymer fresh pastes with the different NaOH content at the early age. *Constr Build Mater.* 261, 120529 (2020). <https://doi.org/10.1016/j.conbuildmat.2020.120529>
56. Dai, X., Aydin, S., Yardimci, M.Y., Lesage, K., De Schutter, G.: Early age reaction, rheological properties and pore solution chemistry of NaOH-activated slag mixtures. *Cem Concr Compos.* 133, 104715 (2022). <https://doi.org/10.1016/j.cemconcomp.2022.104715>
57. Yun, H., Kim, Y.J., Kim, S. Bin, Yoon, H.J., Kwak, S.K., Lee, K.B.: Preparation of copper-loaded porous carbons through hydrothermal carbonization and ZnCl₂ activation and their application to selective CO

- adsorption: Experimental and DFT calculation studies. *J Hazard Mater.* 426, 127816 (2022). <https://doi.org/10.1016/j.jhazmat.2021.127816>
58. Zhao, H., Zhong, H., Jiang, Y., Li, H., Tang, P., Li, D., Feng, Y.: Porous ZnCl₂-Activated Carbon from Shaddock Peel: Methylene Blue Adsorption Behavior. *Materials.* 15, 895 (2022). <https://doi.org/10.3390/ma15030895>
 59. Nassar, H., Zyoud, A., El-Hamouz, A., Tanbour, R., Halayqa, N., Hilal, H.S.: Aqueous nitrate ion adsorption/desorption by olive solid waste-based carbon activated using ZnCl₂. *Sustain Chem Pharm.* 18, 100335 (2020). <https://doi.org/10.1016/j.scp.2020.100335>
 60. Brunauer, S., Emmett, P.H., Teller, E.: Adsorption of Gases in Multimolecular Layers. *J Am Chem Soc.* 60, 309–319 (1938). <https://doi.org/10.1021/ja01269a023>
 61. Barrett, E.P., Joyner, L.G., Halenda, P.P.: The Determination of Pore Volume and Area Distributions in Porous Substances. I. Computations from Nitrogen Isotherms. *J Am Chem Soc.* 73, 373–380 (1951). <https://doi.org/10.1021/ja01145a126>
 62. Jagiello, J., Jaroniec, M.: 2D-NLDFT adsorption models for porous oxides with corrugated cylindrical pores. *J Colloid Interface Sci.* 532, 588–597 (2018). <https://doi.org/10.1016/j.jcis.2018.08.021>
 63. Al-sareji, O.J., Meiczinger, M., Salman, J.M., Al-Juboori, R.A., Hashim, K.S., Somogyi, V., Jakab, M.: Ketoprofen and aspirin removal by laccase immobilized on date stones. *Chemosphere.* 311, 137133 (2023). <https://doi.org/10.1016/j.chemosphere.2022.137133>
 64. Pandey, D., Daverey, A., Dutta, K., Arunachalam, K.: Bioremoval of toxic malachite green from water through simultaneous decolorization and degradation using laccase immobilized biochar. *Chemosphere.* 297, 134126 (2022). <https://doi.org/10.1016/j.chemosphere.2022.134126>
 65. Al-sareji, O.J., Meiczinger, M., Somogyi, V., Al-Juboori, R.A., Grmasha, R.A., Stenger-Kovács, C., Jakab, M., Hashim, K.S.: Removal of emerging pollutants from water using enzyme-immobilized activated carbon from coconut shell. *J Environ Chem Eng.* 11, 109803 (2023). <https://doi.org/10.1016/j.jece.2023.109803>
 66. Boehm, H.P.: Some aspects of the surface chemistry of carbon blacks and other carbons. *Carbon N Y.* 32, 759–769 (1994). [https://doi.org/10.1016/0008-6223\(94\)90031-0](https://doi.org/10.1016/0008-6223(94)90031-0)
 67. Boehm, H. -P., Diehl, E., Heck, W., Sappok, R.: Surface Oxides of Carbon. *Angewandte Chemie International Edition in English.* 3, 669–677 (1964). <https://doi.org/10.1002/anie.196406691>
 68. Langmuir, I.: THE CONSTITUTION AND FUNDAMENTAL PROPERTIES OF SOLIDS AND LIQUIDS. PART I. SOLIDS. *J Am Chem Soc.* 38, 2221–2295 (1916). <https://doi.org/10.1021/ja02268a002>
 69. Freundlich, H.: Adsorption in solution. *Phys Chem Soc.* 40, 1361–1368 (1906)
 70. Lagergren, S.Y.: Zur Theory of sogenannten Adsorption gelöster Stoffe. *Kungliga Svenska Vetenskapsakad Handlingar.* 24, 1–39 (1898)
 71. Ho, Y.S., McKay, G.: Pseudo-second order model for sorption processes. *Process Biochemistry.* 34, 451–465 (1999). [https://doi.org/10.1016/S0032-9592\(98\)00112-5](https://doi.org/10.1016/S0032-9592(98)00112-5)
 72. HO, Y.: Review of second-order models for adsorption systems. *J Hazard Mater.* 136, 681–689 (2006). <https://doi.org/10.1016/j.jhazmat.2005.12.043>
 73. Weber, W.J., Morris, J.C.: Kinetics of Adsorption on Carbon from Solution. *Journal of the Sanitary Engineering Division.* 89, 31–59 (1963). <https://doi.org/10.1061/JSEDAI.0000430>
 74. McKay, G., Blair, H.S., Gardner, J.: The adsorption of dyes in chitin. III. Intraparticle diffusion processes. *J Appl Polym Sci.* 28, 1767–1778 (1983). <https://doi.org/10.1002/app.1983.070280519>
 75. Rudzinski, W., Plazinski, W.: Theoretical description of the kinetics of solute adsorption at heterogeneous solid/solution interfaces. *Appl Surf Sci.* 253, 5827–5840 (2007). <https://doi.org/10.1016/j.apsusc.2006.12.038>
 76. Vargas, D.P., Giraldo, L., Moreno-Piraján, J.C.: Calorimetric study of the CO₂ adsorption on carbon materials. *J Therm Anal Calorim.* 117, 1299–1309 (2014). <https://doi.org/10.1007/s10973-014-3909-x>
 77. Vargas, D.P., Giraldo, L., Moreno-Piraján, J.C.: Accessible area and hydrophobicity of activated carbons obtained from the enthalpy characterization. *Adsorption.* 22, 3–11 (2016). <https://doi.org/10.1007/s10450-015-9721-5>
 78. Moreno, J.C., Giraldo, L.: Calorimetric instrumentation applied to the determination of immersion enthalpies of porous solids. In: Moreno, J.C. (ed.) . In *Porous Solids Preparation, Characterization and Applications* . pp. 281–297. Uniandes, Bogotá (2007)

79. Murillo, Y.S., Giraldo, L., Moreno-Piraján, J.C.: Contribution enthalpic in the interaction of activated carbon with polar and apolar solvents. *Arabian Journal of Chemistry*. 6, 347–351 (2013). <https://doi.org/10.1016/j.arabjc.2012.07.003>
80. Rodríguez, G., Giraldo, L., Moreno, J.C.: Immersion enthalpies of activated carbon fabrics as a physicochemical characterization parameter. *Revista Colombiana de Química*. 38, 435–445 (2009)
81. Moreno-Piraján, J.C., Giraldo, L.: Study of Carbon Foams Synthesized by the Pyrolysis of Wastes Coconut Shells of African Palm at Different Conditions and use of Immersion Calorimetry as a Tool for Characterization. *Oriental Journal Of Chemistry*. 29, 877–887 (2013). <https://doi.org/10.13005/ojc/290305>
82. Hernández-Monje, D., Giraldo, L., Moreno-Piraján, J.: Immersion Enthalpy of Activated Carbon–Cyclohexane and Activated Carbon–Hexane. Difference in the Solid–Liquid Interaction Enthalpy Due to the Structure of the Solvent. *Processes*. 7, 180 (2019). <https://doi.org/10.3390/pr7040180>
83. Hu, J., Yuan, B., Zhang, Y., Guo, M.: Immobilization of laccase on magnetic silica nanoparticles and its application in the oxidation of guaiacol, a phenolic lignin model compound. *RSC Adv*. 5, 99439–99447 (2015). <https://doi.org/10.1039/C5RA14982G>
84. Thommes, M., Kaneko, K., Neimark, A. V., Olivier, J.P., Rodriguez-Reinoso, F., Rouquerol, J., Sing, K.S.W.: Physisorption of gases, with special reference to the evaluation of surface area and pore size distribution (IUPAC Technical Report). *Pure and Applied Chemistry*. 87, 1051–1069 (2015). <https://doi.org/10.1515/PAC-2014-1117/MACHINEREADABLECITATION/RIS>